Industrial Engineering Journal
ISSN: 0970-2555
Volume : 53, Issue 7, July : 2024

Solar based High Gain Bidirectional DC-DC Converter Fed Drive for an Electric Vehicle with Battery Charging Capability During Braking

1.Mr. G. Manik kumar, 2. Dr. T. RAJESH, M. Tech., Scholar, Ph.D., 3. Dr. P. DURAIPANDY, M.E., Ph.D.,

1. M. Tech Student, 2.3. Associate Professor
Department of Electrical and Electronics Engineering,
J.B. Institute of Engineering and Technology, Hyderabad, Telangana – 500 075.

ABSTRACT

The increasing demand for sustainable and efficient transportation solutions has led to significant advancements in electric vehicle (EV) technology. This paper presents a novel approach to enhancing the energy efficiency of EVs through the integration of a solar-based high-gain bidirectional DC-DC converter. This system not only powers the EV drive but also incorporates battery charging capability during braking, thus harnessing regenerative braking energy.

The proposed system employs a high-gain bidirectional DC-DC converter to efficiently manage power flow between the solar panels, the EV's battery, and the drive system. This converter design ensures optimal energy transfer, maximizing the utilization of solar energy while maintaining the necessary power levels for vehicle operation. During braking, the converter facilitates regenerative braking by directing the recovered kinetic energy back into the battery, enhancing the overall energy efficiency and extending the vehicle's range.

The proposed topology makes use of dual current path inductor structures which reduces their size and eliminates the need for an additional clamping circuit to give energy to the load. Without using voltage multiplier cells (VMC) or hybrid switched-capacitor approaches, the proposed converter can achieve a significant voltage gain. The simulation of the proposed converter-based drive is carried out using MATLAB/Simulink the performance analysis is done for different driving conditions. The converter powers the motor through the battery during the forward motoring mode. The motor acts as a generator during regenerative braking and the energy is transferred back through the converter to the battery which stores the recovered energy.

INDEX TERMS bidirectional dc–dc converter, high voltage gain, electric vehicle, regenerative braking, battery charging.

I.INTRODUCTION

Governmental bodies and organizations are enforcing stricter limits for fuel consumption and emissions due to the rising rate of oil consumption in the transportation sector, as well as growing concerns over the impact of global warming and the depletion of energy resources. By 2040, it is predicted that the yearly sales of EVs and Hybrid Electric Vehicles (HEVs) would surpass those of petrol and diesel vehicles, with sales of over 48 million [1]. The automobile industry is concentrating on the development of new technologies for the power train, battery, and charging infrastructure in response to the rising demand for vehicles with better fuel efficiency and less impact on the environment. The installation of a high-energy battery pack and regenerative braking aid in extending the driving range and battery life of electric vehicles.

Power electronic converters find its application in drivetrain to modulate the power flow from battery to the propulsion motors and to facilitate regenerative braking in the reverse direction. To increase efficiency and power density, the drivetrain motor and propulsion inverter are made to operate at higher voltage [2]. To raise the battery voltage to the desired level, a boost converter is used. It also enhances the overall performance of the drivetrain by delinking the battery voltage and the inverter dc link voltage [3]. The DC-DC converter must be bidirectional because the forward mode will face transient and overload conditions during which power gets transferred from the battery to load and during the reverse mode, the battery pack has to get charged. Some of the benefits derived by providing a BDC between the battery and the inverter [4], [5] are: a) It reduces the stress on the inverter with an additional DC stage b) It adjusts the inverter supply voltage to increase the motor output, c) The cost and size of the battery can be reduced because of lower cell count requirement and d) The system voltage and battery can be individually designed by the manufacturers. This architecture thus enables versatile system designs for vehicles with various output characteristics. For instance, the battery nominal voltage in the 2010 Toyota Prius is about 200 V, while the DC-DC converter raises the voltage of the dc bus to about 650 V [2].

The most common BDC is the one with an isolated framework [2], [6] to [11]. These isolated converters employ the high frequency transformer throughout the operation, increasing its losses and volume. Transformer core saturation [25] is another issue with this kind of converter. Additionally, many isolated converter configurations, such as LLC converters, CLLC converters and dual-active-bridge (DAB) converters, which are the most prevalent kind of isolated BDCs, call for a significant number of active switches [10], [11]. Therefore, nonisolated BDCs are typically preferred when isolation is not mandatory. This is as a result of its simple structure and low component count, which draw the attention of several researchers. They are suitable for some applications, such as the drive train of an electric vehicle, where size and weight are crucial considerations.

To attain high conversion ratios, non-isolated BDCs employ many circuit principles, including SEPIC/Cuk/Zeta, voltage multiplier cells, switching capacitors, and linked inductors. Due to their cascaded construction, SEPIC/Cuk/Zeta converters have a low efficiency and higher voltage stress. BDCs can be designed using voltage multiplier cells; however, this is restricted by the high voltage across switches. BDCs [12] to [14] utilize switched capacitors that perform better, have a simpler construction, and require less control complexity. However, for high-gain applications, the circuit becomes progressively complex and is susceptible to losses with the growing number of switches and capacitors.

The system efficiency can be increased with hybrid topologies, but there is insufficient voltage gain and a greater ripple current [15] associated with few of these topologies. However, high conversion factors can be attained using hybrid architectures like SEPIC/quasi-Z source with switched capacitors [16], [17]. Conversion efficiency is nonetheless limited by a high component count and its inability to provide soft switching. Large ripple current at the LV side is a prevalent issue with all high gain non-isolated BDC circuits as it shortens the life and degrade the performance of the battery. Large capacitors can control input ripple current [18], but this is not preferred as the capacitor adds bulk and expense to the system. Interleaved DC-DC converter is a better option to reduce the input current ripple, but it has a lower voltage gain and more components [19].

Another significant advancement in this regard is the coupled inductor-based bidirectional converter (CIBDC) architecture [20-25] that aims to achieve a high voltage conversion ratio. Contrary to transformer-based topologies, these coupled inductor-based systems [20] allow energy exchange at several instants during the course of a single time period. By carefully planning the circuit, switch current and voltage stress can be reduced as well. Clamping the coupled inductor's leakage energy and minimizing voltage spikes and stress across switches are major challenges in coupled inductor topologies. By raising the coupled inductance at the low voltage side, the CIBDC proposed in [21] could minimize the current ripple. But it restricts the number of turns of other windings and in turn the voltage transfer ratio of the BDC. The CIBDC suggested in [24] employs two secondary coupled inductor branches to obtain a greater voltage conversion ratio and current sharing features in addition to soft switching. A non-isolated high gain converter for microgrids is suggested in [26], where coupled inductor is substituted by a normal inductor to make the topology appropriate for high voltage conversion application. However, it is unidirectional. The proposed converter is a modified version of the converter in [26] with bidirectional capability for electric vehicle applications.

The proposed high gain bidirectional converter (HGBDC) utilizes only four active power switches which makes its construction simple. High voltage gain is achieved by choosing the appropriate duty cycle and designing proper inductor and capacitor values. Operation of the converter at a lower duty ratio reduces the core saturation problem of the inductor. Furthermore, the input current is divided among the inductors, which reduces their size and eliminates the need for an additional clamping circuit to give energy to the load. The performance analysis of the converter fed drive has also been carried out using in MATLAB/Simulink and OPAL-RT SIL system to prove the viability of the converter in interfacing energy storage device to the dc link in electric vehicles. The converter successfully controls the power flow from the energy source to the motor and vice versa during forward motoring and regenerative braking.

Simulation results demonstrate that the high-gain bidirectional DC-DC converter significantly improves the energy conversion efficiency and the performance of the EV drive. The system effectively captures and stores regenerative braking energy, reducing the reliance on grid charging and promoting sustainable energy use. The integration of solar power further contributes to the vehicle's energy independence and environmental footprint reduction.
This study underscores the potential of combining advanced power electronics with renewable energy sources in electric vehicle applications. The proposed system offers a promising solution for increasing the efficiency and sustainability of EVs, paving the way for greener and more cost-effective transportation options.

II.DC-DC CONVERTERS

A DC-DC converter with a high step-up voltage, which can be used in various applications like automobile headlights, fuel cell energy conversion systems, solar-cell energy conversion systems and battery backup systems for uninterruptable power supplies.Theoritically, a dc-dc boost converter can attain a high step-up voltage with a high effective duty ratio.But,in practical, the step-up voltage gain is restricted by the effect of power switches and the equivalent series resistance(ESR) of inductors and capacitors.

Generally a conventional boost converter is used to get a high-step-up voltage gain with a large duty ratio. But, the efficiency and the voltage gain are restricted due to the losses of power switches and diodes, the

equivalent series resistance of inductors and capacitors and the reverse recovery problem of diodes. Due to the leakage inductance of the transformer, high voltage stress and power dissipation effected by the active switch of these converters. To reduce the Voltage spike, a resistor-capacitor –diode snubbed can be employed to limit the voltage stress on the active switch. But, these results in reduction of effiency.Based on the coupled inductor; converters with low input ripple current are developed. The low input current ripple of these converters is realized by using an additional LC circuit with a coupled inductor.

III.ELECTRIC VEHICLE

An **electric vehicle**, also called an **EV**, uses one or more electric motors or traction motors for propulsion. An electric vehicle may be powered through a collector system by electricity from off-vehicle sources, or may be self-contained with a battery, solar panels or an electric generator to convert fuel to electricity.[1] EVs include, but are not limited to, road and rail vehicles, surface and underwater vessels, electric aircraft and electric spacecraft.

EVs first came into existence in the mid-19th century, when electricity was among the preferred methods for motor vehicle propulsion, providing a level of comfort and ease of operation that could not be achieved by the gasoline cars of the time. Modern internal combustion engines have been the dominant propulsion method for motor vehicles for almost 100 years, but electric power has remained commonplace in other vehicle types, such as trains and smaller vehicles of all types.

In the 21st century, EVs saw a resurgence due to technological developments, and an increased focus on renewable energy. A great deal of demand for electric vehicles developed and a small core of do-it-yourself (DIY) engineers began sharing technical details for doing electric vehicle conversions. Government incentives to increase adoptions were introduced, including in the United States and the European Union

IV.PROPOSED HIGH GAIN BIDIRECTIONAL DC-DC CONVERTER (HGBDC)

The proposed HGBDC shown in figure 1 has four active power switches (S1, S2, S3, and S4), two identical inductors (L1 and L2), a diode (D1), and a capacitor (CH) at the high voltage side. Diode D1 helps in blocking the reverse voltage VL appearing across the MOSFET while the switches S1 and S2 are conducting in

boost mode. A switching frequency of fs is used by the switches S1, S2, S3, and S4. During boost mode, switches S1 and S2 have a duty ratio of d1, and switch S3 has a duty ratio of d2. The duty ratio of the switch S4 is (1- d1-d2) during boost mode and it is db during buck mode of operation of the converter.

A. OPERATION OF THE HGBDC IN BOOST MODE

The boost operation of the converter is explained in three different phases namely, Mode I, Mode II and Mode III. The current flow path of the proposed HGBDC operating in boost mode is depicted in figure 2. During this mode, the energy is transferred from the low voltage side to the high voltage side of the converter with the help of controlled switches S1, S2, S3 and S4. The switches S1, S2 and S3 are operated through the PWM control. Typical waveforms of the proposed HGBDC in boost mode for continuous conduction are shown in figure 3.

1) MODE I

The switches S1 and S2 are turned on in this mode (t0, t1), while the switches S3 and S4 are

Industrial Engineering Journal
ISSN: 0970-2555
Volume : 53, Issue 7, July : 2024

turned off for the duration of d1Ts. Energy flow is from the battery to the inductors L1, L2 which are connected in parallel, as shown in figure 2(a). The energy stored in the capacitor; CH is released to the load. The voltage across the inductors is expressed in (1) to (3).

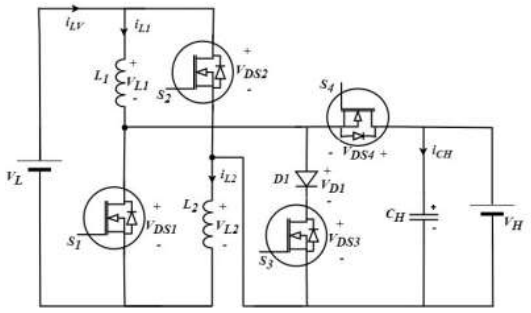

FIGURE 1. Proposed High Gain Bidirectional DC -DC Converter (HGBDC)

$$v_{L1} = v_{L2} = V_L \quad (1)$$

$$L_1 \frac{di_{L1}}{dt} = L_2 \frac{di_{L2}}{dt} = L \frac{di_L}{dt} = V_L \quad (2)$$

$$\frac{di_L}{dt} = \frac{V_L}{L} \quad (3)$$

where vL1 and vL2 are the voltages across inductors L1 and L2 respectively .

2) MODE II

Switch S3 is active for the duration of d2Ts, while switches S1 and S2 are turned off in Mode II (t1, t2). As displayed in figure 2(b), current flow is through L1, D1, S3 and L2. The energy from the source is delivered to the inductors. The load receives the energy that is stored in the capacitor. Source is in series with the inductors in this mode. Equations (4) and (5) represent the currents flowing through and the voltages across the inductors.

$$i_{L1} = i_{L2} \quad (4)$$

where iL1 and iL2 are the current through inductors L1 and L2 respectively .

$$v_{L1} + v_{L2} = V_L \quad (5)$$

$$v_{L1} = v_{L2} = L \frac{di_L}{dt} \quad (6)$$

$$\frac{di_L}{dt} = \frac{V_L}{2L} \quad (7)$$

3) MODE III

The MOSFET switches S1, S2 and S3 are turned off in this mode (t2, t3), whereas the body diode of the MOSFET S4 conducts during (1-d1-d2)TS. Diode D1 is reverse biased. The load is supplied by both the source and the inductors as depicted in figure 2(c). The capacitor CH is in charging mode as the body diode of S4 is forward biased. The inductors are connected in series to the source. The current through and the voltage across the inductors are given in (8) to (10).

$$i_{L1} = i_{L2} \quad (8)$$

$$v_{L1} + v_{L2} = V_L - V_H \quad (9)$$

$$v_{L1} = v_{L2} = L \frac{di_L}{dt} \quad (10)$$

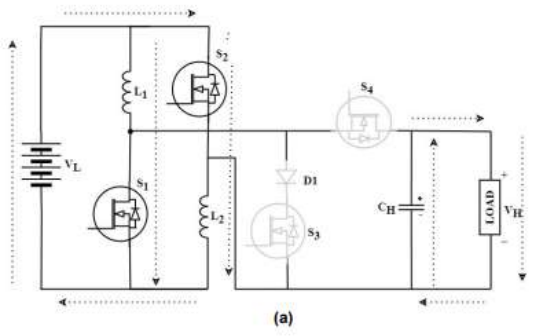

(a)

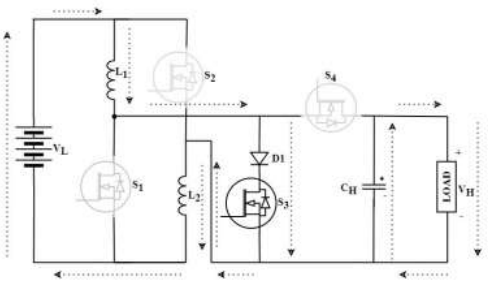

(b)

Industrial Engineering Journal
ISSN: 0970-2555
Volume : 53, Issue 7, July : 2024

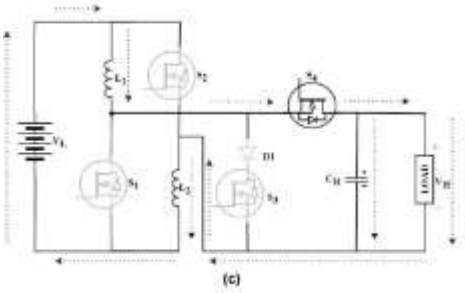

FIGURE 2. HGBDC in boost mode (a) Mode I (b) Mode II (c) Mode III

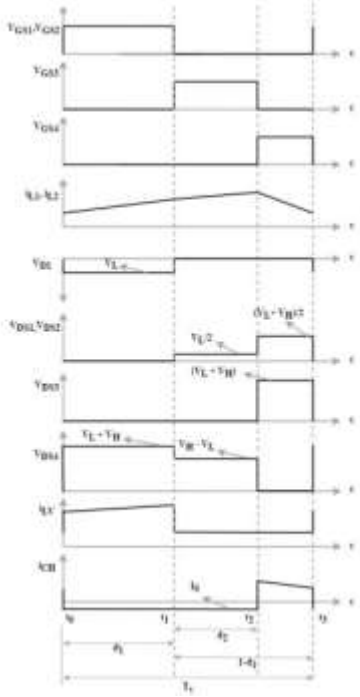

FIGURE 3. Operational waveforms of HGBDC in boost mode (CCM)

From (9) and (10),

$$\frac{di_L}{dt} = \frac{V_L - V_H}{2L} \qquad (11)$$

(3), (7), and (11) are combined to get (12) using the state space averaging technique:

$$\int_0^{d_1 T_s} \left(\frac{di_L}{dt}\right)^{I} dt + \int_0^{d_2 T_s} \left(\frac{di_L}{dt}\right)^{II} dt + \int_0^{(1-d_1-d_2)T_s} \left(\frac{di_L}{dt}\right)^{III} dt = 0 \qquad (12)$$

The modes of operation are indicated by the superscripts I, II, and III. The resulting voltage gain is given by (13).

$$\frac{V_H}{V_L} = \frac{(1+d_1)}{(1-d_1-d_2)} \qquad (13)$$

B. OPERATION OF THE PROPOSED HGBDC IN BUCK MODE

The buck operation of the converter is explained in two different phases during the same switching cycle. The current flow path of the proposed HGBDC operating in buck mode is depicted in figure 4. Energy is transferred from the high voltage side to the low voltage side with the help of controlled switches S4, S1 and S2 in this mode. The switch S4 is operated through the PWM control with a duty ratio of db. Operational waveforms of the proposed HGBDC in buck mode for continuous conduction mode (CCM) are depicted in figure 5.

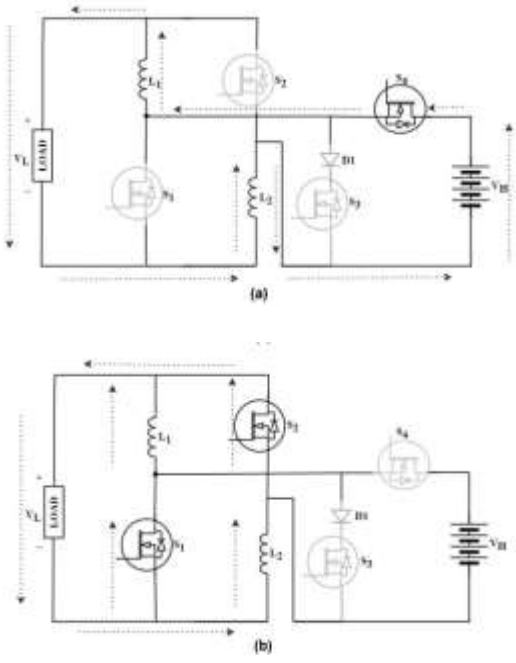

FIGURE 4. HGBDC in buck mode (a) Mode I (b) Mode II

1) MODE I

Industrial Engineering Journal
ISSN: 0970-2555
Volume : 53, Issue 7, July : 2024

In this mode (t0, t1), S4 is turned on and S1/S2/S3 are turned off for a duration of dbTs . The inductors L1 and L2, which are connected in series with the load and the battery, facilitate the transfer of energy from the high voltage side to the low voltage side of the converter as shown in figure 4(a). Equations (14) to (16) give the current flowing through and the voltage across the inductors in this mode.

$$i_{L1} = i_{L2} \quad (14)$$

$$v_{L1} + v_{L2} = V_H - V_L \quad (15)$$

$$v_{L1} = v_{L2} = L\frac{di_L}{dt}$$

$$\frac{di_L}{dt} = \frac{V_H - V_L}{2L} \quad (16)$$

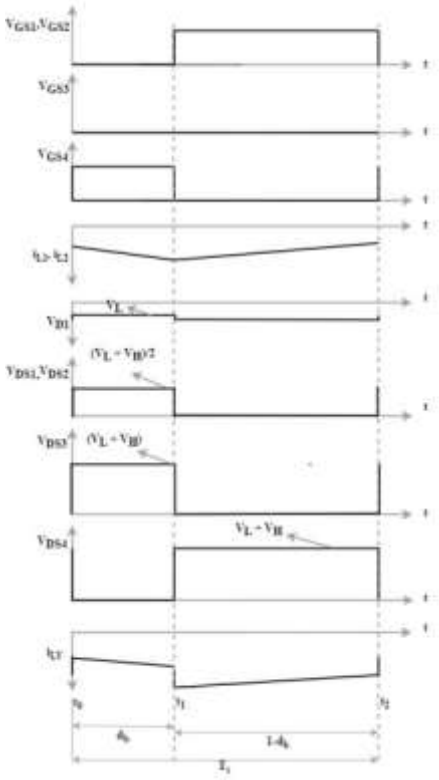

FIGURE 5. Operational waveforms of HGBDC in buck mode (CCM)

2) MODE II

The body diodes of the MOSFETs S1 and S2 conduct for a duration of (1 − db)Ts in this mode (t1, t2), while the MOSFET S4 is turned off. Figure 4(b) depicts the current flow path. Inductors L1 and L2 discharge their stored energy to the load on low voltage side. Because L1 and L2 are in parallel, the voltages across them are as given in (17).

$$v_{L1} = v_{L2} = -V_L \quad (17)$$

$$L\frac{di_{L1}}{dt} = L\frac{di_{L2}}{dt} = -V_L \quad (18)$$

$$\frac{di_L}{dt} = \frac{-V_L}{L} \quad (19)$$

Equations (16) and (19) are combined to get (20) using the state space averaging technique.

$$\int_0^{d_b T_s}\left(\frac{di_L}{dt}\right)^{I} dt + \int_0^{(1-d_b)}\left(\frac{di_L}{dt}\right)^{II} dt = 0 \quad (20)$$

The modes of operation are indicated by the superscripts I and II. The resulting voltage gain in buck mode is given by (21)

$$\frac{V_L}{V_H} = \frac{d_b}{(2-d_b)} \quad (21)$$

Where, db is the duty ratio of the HGBDC in buck mode of operation.

C. EFFICIENCY ANALYSIS

In order to determine the theoretical efficiency curve and compute converter losses, the efficiency of the proposed converter is derived by taking the parasitic elements into consideration. To make the mathematical analysis simpler, the ripple in the capacitor voltage and inductor current is ignored. The expression for voltage VH at the high voltage side of the converter, by taking these parasitic elements into consideration is given by (22)

$$V_H = \frac{V_L(1+d_1) - V_{D1}d_2}{\left(\frac{2(d_1\alpha_1 + d_2\alpha_2 + (1-d_1-d_2)\alpha_3)}{R_H(1-d_1-d_2)}\right) + (1-d_1-d_2)} \quad (22)$$

$$\begin{cases} \alpha_1 = r_{S1} + r_{L1} \\ \alpha_2 = \dfrac{(r_{S3} + r_{L1} + r_{L2} + r_{D1})}{2} \\ \alpha_3 = \dfrac{(r_{L1} + r_{L2} + r_{S4})}{2} \end{cases}$$

Where, rL1 and rL2 are the ESR of the inductors L1 and L2 respectively. Similarly, rS1, rS2, rS3 and rS4 represent the ON state

Industrial Engineering Journal
ISSN: 0970-2555
Volume : 53, Issue 7, July : 2024

resistances of the switches S1, S2, S3 and S4 respectively. rD1 and VD1 are the internal resistance and the voltage drop across the diode D1 respectively. The resulting equation for efficiency of the proposed converter in boost mode of operation is given in (23).

$$\eta = \frac{P_H}{P_L} = \frac{\left(\frac{V_H^2}{R_H} - P_{SW}\right)}{\frac{V_L V_H (1+d_1)}{R_H (1-d_1-d_2)}} \quad (23)$$

Where PH and PL are the power at high voltage side and low voltage side of the converter respectively. RH is the load resistance at high voltage side. PSW is the switching loss across the power switches which is given by (24). The rise and fall time of the power switches are represented by tr and tf respectively

$$P_{SW} = 0.5 V_{DS} I_D (t_r + t_f) f_{SW} \quad (24)$$

The expression for voltage VL at the low voltage side of the converter, by taking the parasitic elements into consideration is given in (25).

$$V_L = \left(\frac{d_b}{2-d_b}\right) \frac{(2-d_b)^2 R_L}{(2-d_b)^2 R_L + d_b \beta_1 + 2(1-d_b)\beta_2} \quad (25)$$

Where

$$\begin{cases} \beta_1 = r_{S4} + r_{L1} + r_{L2} \\ \beta_2 = r_{L1} + r_{S1} \end{cases}$$

he calculated efficiency of the proposed converter in stepdown mode is given by (26).

$$\eta = \frac{P_L}{P_H} = \frac{\left(\frac{V_L^2}{R_L} - P_{SW}\right)}{\frac{d_b V_L V_H}{d_b (2-d_b) R_L}} \quad (26)$$

Where RL is the load resistance at low voltage side.

V.CONVERTER DESIGN AND MOTOR CONTROL

The proposed HGBDC may be used to test its viability for applications like electric automobiles by integrating it into a simple DC motor drive. In this work, the converter is operated in continuous conduction mode to drive the dc motor in forward motoring and regenerative braking modes. The HGBDC is connected to a battery and a dc motor load as shown in figure 8. The light electric vehicle industry makes extensive use of DC motors, which are chosen for their simplicity and to check the viability of the converter operation in the proposed scheme. A 5 HP separately excited DC motor model rated at 240 V and 1750 rpm is utilized as the load to analyze the performance of the HGBDC in both MATLAB/Simulink and the OP4500 real-time simulation mode. The converter specifications are given in Table III. The simulation makes use of the lithium ion (Li-ion) battery, whose specifications are listed in Table IV. The lithium-ion battery has a strong possibility of replacing other batteries as the foreseeable future of electric vehicle batteries. This is due to its fascinating properties including large power density, high energy density, extended life cycle, absence of memory effect, and superior energy efficiency. During regenerative braking, the proposed BDC transfers power from the motor back to the battery, and when the vehicle is moving, it delivers power from the battery to the DC motor.

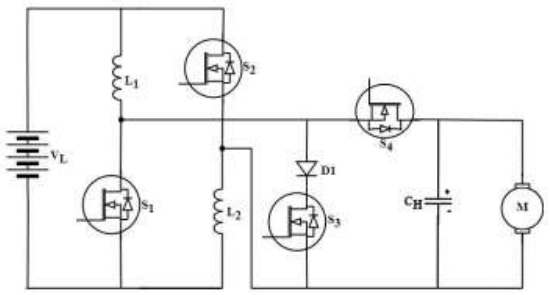

FIGURE 8. HGBDC connected to battery source and a dc motor load.

A. INDUCTOR DESIGN

The selection of an inductor is influenced by the motoring mode of operation, which in turn depends on the input voltage (VL), current

Industrial Engineering Journal
ISSN: 0970-2555
Volume : 53, Issue 7, July : 2024

ripple (ΔiL), frequency of switching (fs), and the duty cycle (d1). The critical inductance value for the operation of the proposed HGBDC in CCM is determined using (27).

$$L_{1,critical} = L_{2,critical} = \frac{V_L d_1}{\Delta i_L f_s} \quad (27)$$

The inductor has been designed with 50 kHz switching frequency and a specified current ripple which is considered as 12% of the input current here.

B. CAPACITOR DESIGN

The rated power (Po) of the converter, load voltage (Vo), ripple voltage (ΔVc), and the frequency of switching (fs), are used to calculate the value of the capacitor, CH on the high voltage side using (28).

$$C_{o,critical} = \frac{P_o}{V_o \Delta V_c f_s} \quad (28)$$

A voltage ripple of 1% of the output voltage, VH is used for the design of the capacitor.

C. VOLTAGE STRESS OF THE SWITCH AND DIODE

The voltage stress VDS1, VDS2, VDS3 and VDS4 across switches S1 and S2, S3 and S4 for boost mode of operation are given by (29), (30) and (31).

$$V_{DS1} = V_{DS2} = \frac{V_H + V_L}{2} \quad (29)$$
$$V_{DS3} = V_H \quad (30)$$
$$V_{DS4} = V_H + V_L \quad (31)$$

The voltage stress VD1 on the diode D1 for both buck and boost mode of operations are given by equation (31).

$$V_{D1} = V_L + V_H \quad (32)$$

The voltage stress VDS1, VDS2, VDS3 and VDS4 across switches S1 and S2, S3 and S4 for buck operation are given in (33) and (34).

$$V_{DS1} = V_{DS2} = \frac{V_H + V_L}{2} \quad (33)$$
$$V_{DS3} = V_{DS4} = V_H + V_L \quad (34)$$

TABLE III CONVERTER SPECIFICATIONS

Parameter	MATLAB/Simulink	RT-LAB
Input Voltage	48V	48V
Output Voltage	240V	240V
Switching Frequenc	50 kHz	5 kHz
Inductor L_1, L_2	200 µH	1000 µH
Capacitor C_H	300 µF	1000 µF
Load (DC motor)	5 HP, 240 V, 1750rpm	5 HP, 240 V, 1750 rpm

TABLE IV BATTERY PARAMETERS

Parameter	Value/Specifications
Type	Li-ion
Nominal Voltage	48 V
Initial %SoC	80
Battery Capacity	140 Ah
Nominal Discharge Current	60.87 A

D. CONTROL TECHNIQUE

A practical technique for adjusting the speed of the drive is to control the output voltage of the BDC. A PID controller is used to ensure that the vehicle reaches the target speed and reacts quickly to rapid changes in speed without oscillations. Figure 9 depicts the control circuitry for the HGBDC. It senses the motor speed $\omega motor$ and compares it to the reference speed ωref. The error signal is processed by the PID controller and compared to a high frequency sawtooth signal to generate the PWM control signals.

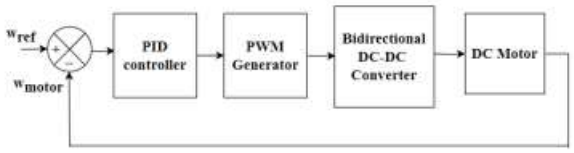

FIGURE 9. Block diagram of closed loop control scheme

VI.MODELLING AND SIMULATION

The HGBDC fed DC motor drive is modelled and simulated using MATLAB/Simulink for a

duration of 10 seconds. The steady-state inductor current and the gate drive pulses of the MOSFET switches for both boost and buck mode of operations of the converter are shown in figure 10 and figure 11 respectively. In boost (forward motoring) mode, the inductor current increases when the first three switches S1, S2 and S3 are turned on, whereas the current through the inductor decreases when the switch S4 is turned on. As shown in figure 10, the average value of the inductor current in steady state is 32 A. During buck (regenerative braking) mode, the steady-state inductor current is -13.5A. Negative value of the inductor current shows the reversal of current flow from the load to source; hence the power flow. Battery is charged from the regenerative power during this braking mode. For a rated speed of 1750 rpm in forward motoring mode, the duty ratio of the PWM pulses generated by the PWM controller, d1 and d2 for the switches S1/S2 and S3 respectively are 0.455 and 0.245 for a voltage gain of 4.85. During regenerative braking mode, the switch S4 operates with a duty ratio db which is 0.5 and the corresponding voltage gain is 1/3 for a speed of 1150 rpm.

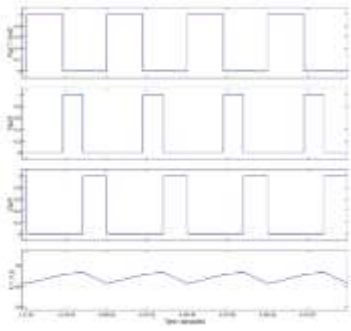

FIGURE 10. Switching signals for S1, S2, S3, S4 and inductor currents in boost mode of operation.

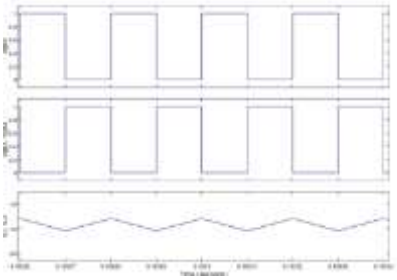

FIGURE 11. Switching signals for S1, S2, S3, S4 and inductor currents in boost mode of operation.

Two different cases are considered for analyzing the dynamics of the system:

(i) transition of the motor operation from forward motoring to regenerative braking.

(ii) a step change in speed during forward motoring.

SIMULATION RESULTS

The Simulink models of the battery, converter, motor, and associated control circuit are integrated with RT-Lab blocks and are accessible on the host computer which is linked to the OP4500 simulation target through a Transmission Control Protocol (TCP)/Internet Protocol (IP) communication network. The OP4500 simulation target performs real-time computations for model inputs and outputs. To analyze the dynamics of the system, a step change in torque is applied and the forward motoring and regenerative braking modes are realized. Also, the impact of variation in speed during forward motoring mode is analyzed. The converter operating frequency is limited to 5 kHz to make it compatible with the existing RT-LAB platform.

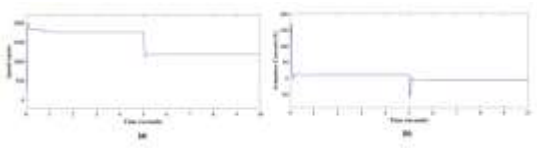

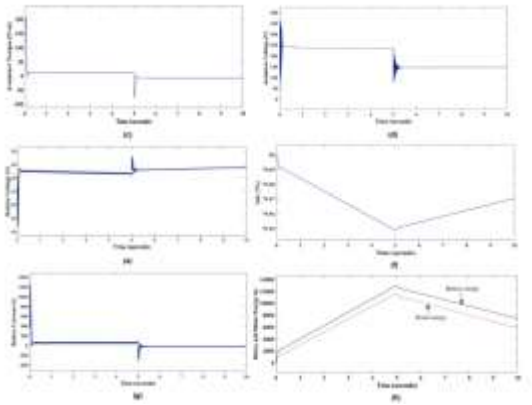

FIGURE 12. Simulation results for case1- Transition of the motor from forward motoring to regenerative braking: (a) speed, (b) armature current, (c) armature torque, (d) armature (output) voltage of the motor, (e) battery voltage and (f) battery SoC (g) battery current (h) battery and motor energy

VII.CONCLUSION

This paper has presented an innovative approach to enhancing the energy efficiency and sustainability of electric vehicles (EVs) through the integration of a solar-based high-gain bidirectional DC-DC converter. This paper focused on the design and development of a High Gain Bidirectional Converter (HGBDC) for electric vehicle applications with battery charging capability during regenerative braking. The performance analysis of the converter is carried out during motoring and regenerative braking modes in MATLAB/Simulink. The proposed method is simpler and the converter can attain high gain with the help of two duty cycle operation. It demonstrates a good balance among the voltage gain and the component counts which gives a viable solution to the application of interfacing storage devices to the DC link in electric vehicles which is the focus of the paper. The HGBDC also successfully controls the power flow direction by modifying the converter's working mode from motoring to regenerative braking. The efficiency of the proposed converter can further be improved by selecting SiC based power switches. Further Soft switching can be implemented to reduce the switching losses when the converter operates at higher frequency, but it adds complexity and increases the number of components.

REFERENCES

[1] C. H. T. Lee, W. Hua, T. Long, C. Jiang and L. V. Iyer, "A Critical Review of Emerging Technologies for Electric and Hybrid Vehicles," IEEE Open Journal of Vehicular Technology, vol. 2, pp. 471-485, 2021, doi: 10.1109/OJVT.2021.3138894.

[2] V. Rathore, K. Rajashekara, P. Nayak and A. Ray, "A High-Gain Multilevel dc–dc Converter for Interfacing Electric Vehicle Battery and Inverter," IEEE Transactions on Industry Applications, vol. 58, no. 5, pp. 6506-6518, Sept.-Oct. 2022, doi: 10.1109/TIA.2022.3185183.

[3] H. Chen, H. Kim, R. Erickson and D. Maksimović, "Electrified Automotive Powertrain Architecture Using Composite DC–DC Converters," IEEE Transactions on Power Electronics, vol. 32, no. 1, pp. 98-116, Jan. 2017, doi: 10.1109/TPEL.2016.2533347.

[4] A. Gupta, R. Ayyanar and S. Chakraborty, "Novel Electric Vehicle Traction Architecture With 48 V Battery and Multi-Input, High Conversion Ratio Converter for High and Variable DC-Link Voltage," IEEE Open Journal of Vehicular Technology, vol. 2, pp. 448-470, 2021, doi: 10.1109/OJVT.2021.3132281.

[5] J. O. Estima and A. J. Marques Cardoso, "Efficiency Analysis of Drive Train Topologies Applied to Electric/Hybrid Vehicles," IEEE Transactions on Vehicular Technology, vol. 61, no. 3, pp. 1021- 1031, March 2012, doi: 10.1109/TVT.2012.2186993.

[6] D. Sha, D. Chen and J. Zhang, "A Bidirectional Three-Level DC– DC Converter with Reduced Circulating Loss and Fully ZVS Achievement for Battery Charging/Discharging," IEEE Journal of Emerging and Selected Topics in Power Electronics, vol. 6, no. 2, pp. 993-1003, June 2018, doi: 10.1109/JESTPE.2017.2778039.

[7] T. Zhu, F. Zhuo, F. Zhao, F. Wang, H. Yi and T. Zhao, "Optimization of Extended Phase-Shift Control for Full-Bridge CLLC Resonant Converter with Improved Light-Load Efficiency," IEEE Transactions on Power Electronics, vol. 35, no. 10, pp. 11129-11142, Oct. 2020, doi: 10.1109/TPEL.2020.2978419.

[8] Y. Shen, H. Wang, A. Al-Durra, Z. Qin and F. Blaabjerg, "A Bidirectional Resonant DC–DC Converter Suitable for Wide Voltage Gain Range," IEEE Transactions on Power Electronics, vol. 33, no. 4, pp. 2957-2975, April 2018, doi: 10.1109/TPEL.2017.2710162.

[9] C. Bai, B. Han, B. -H. Kwon and M. Kim, "Highly Efficient Bidirectional Series-Resonant DC/DC Converter Over Wide Range of Battery Voltages," IEEE Transactions on Power Electronics, vol. 35, no. 4, pp. 3636-3650, April 2020, doi: 10.1109/TPEL.2019.2933408.

[10] N. Hou and Y. W. Li, "Overview and Comparison of Modulation and Control Strategies for a Nonresonant Single-Phase DualActive-Bridge DC–DC Converter," IEEE Transactions on Power Electronics, vol. 35, no. 3, pp. 3148-3172, March 2020, doi: 10.1109/TPEL.2019.2927930.

[11] F. Zahin, A. Abasian and S. A. Khajehoddin, "An Alternative Dual Active Bridge Modulation to Minimize RMS Current and Extend ZVS Range," 2020 IEEE Energy Conversion Congress and Exposition (ECCE), Detroit, MI, USA, 2020, pp. 5952-5959, doi: 10.1109/ECCE44975.2020.9235374.

[12] Y. Zhang, W. Zhang, F. Gao, S. Gao and D. J. Rogers, "A Switched Capacitor Interleaved Bidirectional Converter with Wide Voltage Gain Range for Super Capacitors in EVs," IEEE Transactions on Power Electronics, vol. 35, no. 2, pp. 1536-1547, Feb. 2020, doi: 10.1109/TPEL.2019.2921585.

[13] Y. Zhang, Y. Gao, L. Zhou and M. Sumner, "A Switched-Capacitor Bidirectional DC–DC Converter with Wide Voltage Gain Range for Electric Vehicles with Hybrid Energy Sources," IEEE Transactions on Power Electronics, vol. 33, no. 11, pp. 9459-9469, Nov. 2018, doi: 10.1109/TPEL.2017.2788436.

[14] H. S. H. Chung, W. C. Chow, S. Y. R. Hui and S. T. S. Lee, "Development of a switched-capacitor DC-DC converter with bidirectional power flow," IEEE Transactions on Circuits and Systems I: Fundamental Theory and Applications, vol. 47, no. 9, pp. 1383-1389, Sept. 2000, doi: 10.1109/81.883334.

[15] D. Flores Cortez, G. Waltrich, J. Fraigneaud, H. Miranda and I. Barbi, "DC–DC Converter for Dual-Voltage Automotive Systems Based on Bidirectional Hybrid Switched-Capacitor Architectures," IEEE Transactions on Industrial Electronics, vol. 62, no. 5, pp. 3296-3304, May 2015, doi: 10.1109/TIE.2014.2350454.

[16] Y. Zhang, Q. Liu, Y. Gao, J. Li and M. Sumner, "Hybrid Switched Capacitor/Switched-Quasi-Z-Source Bidirectional DC–DC Converter with a Wide Voltage Gain Range for Hybrid Energy Sources EVs," IEEE Trans. on Ind. Electron., vol. 66, no. 4, pp. 2680-2690, April 2019.doi: 10.1109/TIE.2018.2850020.

[17] Avneet Kumar, Xiaogang Xiong, Xuewei Pan and Motiur Reza, "A Wide Voltage Gain

Bidirectional DC–DC Converter Based on Quasi Z-Source and Switched Capacitor Network" IEEE Transactions on Circuits and Systems II: Express Briefs, Volume: 68, Issue: 4, April 2021, doi: 10.1109/TCSII.2020.3033048.

[18] Z. Wang, P. Wang, B. Li, X. Ma and P. Wang, "A Bidirectional DC–DC Converter with High Voltage Conversion Ratio and Zero Ripple Current for Battery Energy Storage System," IEEE Transactions on Power Electronics, vol. 36, no. 7, pp. 8012-8027, July 2021, doi: 10.1109/TPEL.2020.3048043.

[19] Y. Zhang, Y. Gao, J. Li and M. Sumner, "Interleaved Switched Capacitor Bidirectional DC-DC Converter with Wide Voltage-Gain Range for Energy Storage Systems," IEEE Transactions on Power Electronics, vol. 33, no. 5, pp. 3852-3869, May 2018, doi: 10.1109/TPEL.2017.2719402

[20] L. -S. Yang and T. -J. Liang, "Analysis and Implementation of a Novel Bidirectional DC–DC Converter," IEEE Transactions on Industrial Electronics, vol. 59, no. 1, pp. 422-434, Jan. 2012, doi: 10.1109/TIE.2011.2134060.

[21] A. R. N. Akhormeh, K. Abbaszadeh, M. Moradzadeh and A. Shahirinia, "High-Gain Bidirectional Quadratic DC–DC Converter Based on Coupled Inductor With Current Ripple Reduction Capability," IEEE Transactions on Industrial Electronics, vol. 68, no. 9, pp. 7826-7837, Sept. 2021, doi: 10.1109/TIE.2020.3013551.

[22] B. Li, P. Wang, Z. Wang, X. Ma and H. Bi, "A New Coupled Inductor-Based High-Gain Interleaved DC-DC Converter With Sustained Soft Switching," IEEE Transactions on Vehicular Technology, vol. 70, no. 7, pp. 6527-6541, July 2021, doi: 10.1109/TVT.2021.3083317.

[23] Y. Zhang, H. Liu, J. Li and M. Sumner, "A Low-Current Ripple and Wide Voltage-Gain Range Bidirectional DC–DC Converter with Coupled Inductor," IEEE Trans. on Power Electron., vol. 35, no. 2, pp. 1525-1535, Feb. 2020, doi: 10.1109/TPEL.2019.2921570.

[24] S. M. P., M. Das and V. Agarwal, "Design and Development of a Novel High Voltage Gain, High-Efficiency Bidirectional DC–DC Converter for Storage Interface," IEEE Trans. on Ind. Electron., vol. 66, no. 6, pp. 4490-4501, June 2019, doi: 10.1109/TIE.2018.2860539.

[25] S. B. Santra, D. Chatterjee and T. -J. Liang, "High Gain and High Efficiency Bidirectional DC–DC Converter With Current Sharing Characteristics Using Coupled Inductor," IEEE Transactions on Power Electronics, vol. 36, no. 11, pp. 12819-12833, Nov. 2021, doi: 10.1109/TPEL.2021.3077584.

[26] M. Lakshmi and S. Hemamalini, "Nonisolated High Gain DC–DC Converter for DC Microgrids," IEEE Transactions on Industrial Electronics, vol. 65, no. 2, pp. 1205-1212, Feb. 2018, doi: 10.1109/TIE.2017.2733463.